Canadian Association of Radiologists Journal 67 (2016) 395–401

CANADIAN ASSOCIATION OF RADIOLOGISTS JOURNAL

www.carjonline.org

Abdominal Imaging / Imagerie abdominale

Utility of Diffusion-Weighted MRI to Detect Changes in Liver Diffusion in Benign and Malignant Distal Bile Duct Obstruction: The Influence of Choice of b-Values

Belgin Karan, MD[a,b,*], Gurcan Erbay, MD[a], Zafer Koc, MD[a], Aysin Pourbagher, MD[a], Sedat Yildirim, MD[c], Ahmet Muhtesem Agildere, MD[a]

[a]*Department of Radiology, Baskent University School of Medicine, Adana, Turkey*
[b]*Department of Radiology, Medipol University School of Medicine, Istanbul, Turkey*
[c]*Department of General Surgery, Baskent University School of Medicine, Ankara, Turkey*

Abstract

Purpose: The study sought to evaluate the potential of diffusion-weighted magnetic resonance imaging to detect changes in liver diffusion in benign and malignant distal bile duct obstruction and to investigate the effect of the choice of b-values on apparent diffusion coefficient (ADC).
Methods: Diffusion-weighted imaging was acquired with b-values of 200, 600, 800, and 1000 s/mm^2. ADC values were obtained in 4 segments of the liver. The mean ADC values of 16 patients with malignant distal bile duct obstruction, 14 patients with benign distal bile duct obstruction, and a control group of 16 healthy patients were compared.
Results: Mean ADC values for 4 liver segments were lower in the malignant obstruction group than in the benign obstruction and control groups using b = 200 s/mm^2 ($P < .05$). Mean ADC values of the left lobe medial and lateral segments were lower in the malignant obstruction group than in the benign obstructive and control groups using b = 600 s/mm^2 ($P < .05$). Mean ADC values of the right lobe posterior segment were lower in the malignant and benign obstruction groups than in the control group using b = 1000 s/mm^2 ($P < .05$). Using b = 800 s/mm^2, ADC values of all 4 liver segments in each group were not significantly different ($P > .05$). There were no correlations between the ADC values of liver segments and liver function tests.
Conclusion: Measurement of ADC shows good potential for detecting changes in liver diffusion in patients with distal bile duct obstruction. Calculated ADC values were affected by the choice of b-values.

Résumé

But : L'étude vise à évaluer le potentiel de l'imagerie par résonance magnétique (IRM) de diffusion pour détecter les variations de la diffusion dans le foie de tumeurs malignes et bénignes obstruant l'extrémité distale du canal cholédoque. Elle étudie également l'effet du choix des valeurs de facteur b sur le calcul du coefficient de diffusion apparent (CDA).
Méthodes : Acquisition d'IRM de diffusion à partir de valeurs de facteur b de 200, 600, 800 et 1 000 s/mm^2. Des valeurs du CDA ont été obtenues dans quatre segments du foie. Les valeurs moyennes de 16 patients présentant une tumeur maligne obstruant l'extrémité distale du canal cholédoque, de 14 patients présentant une tumeur bénigne obstruant l'extrémité distale du canal cholédoque et d'un groupe de contrôle formé de 16 patients en bonne santé ont été comparées.
Résultats : Les valeurs moyennes du CDA dans les quatre segments étaient inférieures pour le groupe de patients présentant une obstruction par tumeur maligne comparativement aux deux autres groupes avec une valeur de facteur b de 200 s/mm^2 ($P < 0,05$). Les valeurs moyennes du CDA dans les segments médial et latéral du lobe gauche étaient inférieures pour le groupe de patients présentant une obstruction par tumeur maligne comparativement aux deux autres groupes avec une valeur de facteur b de 600 s/mm^2 ($P < 0,05$). Les valeurs moyennes du CDA dans le segment postérieur du lobe droit étaient inférieures pour les groupes de patients présentant une obstruction par tumeur maligne et par tumeur bénigne comparativement au groupe de contrôle avec une valeur de facteur b de 1 000 s/mm^2 ($P < 0,05$). À une valeur de facteur b de 800 s/mm^2, les valeurs du CDA des quatre segments n'affichaient pas de différence significative selon le groupe ($P > 0,05$). Il n'y avait pas de corrélation entre les valeurs du CDA des segments du foie et les résultats des épreuves de la fonction hépatique.

* Address for correspondence: Belgin Karan, MD, Department of Radiology, Medipol University School of Medicine, Tevfik Bey Mah. Maslak Cesme Cad. Sefakoy, Kucukcekmece/Istanbul, Turkey.

E-mail address: belgink8@yahoo.com (B. Karan).

http://dx.doi.org/10.1016/j.carj.2016.03.006

Conclusion : La mesure du CDA présente un bon potentiel de détection des changements de la diffusion dans le foie chez les patients qui présentent une obstruction de l'extrémité distale du canal cholédoque. Le choix des valeurs de facteur b a influé sur les valeurs calculées du CDA.

Key Words: Biliary obstruction; Diffusion-weighted imaging; Liver fibrosis; Magnetic resonance imaging; b-value

Obstructive jaundice may induce liver and kidney dysfunction, infection, and multiple organ failure [1]. During obstruction, the liver undergoes functional and biochemical changes [2,3]. Bile duct obstruction leads to a reduction in bile flow. Elevation of potentially toxic bile acid in the liver and the blood cause rapid hepatocellular injury and over time, inflammation, bile duct proliferation, and fibrosis can occur [4]. Magnetic resonance imaging (MRI) has been used to evaluate the effects of biliary obstruction on the liver parenchyma: Liver segments associated with intrahepatic biliary obstruction show increased signal intensity on T1-weighted imaging, reflecting a probable change in tissue composition [5,6]. Diffusion-weighted imaging (DWI) is a technique that characterised water molecule diffusion in vivo. In biological tissue, diffusion is quantified by the apparent diffusion coefficient (ADC). However, in vivo, ADC is also affacted by capillary perfusion. Thus, DWI provides information on perfusion and diffusion simultaneously in biological tissue [7,8]. Currently, DWI is used for liver lesion detection and characterisation in combination with T2-weighted and contrast-enhanced MRI [9–11]. DWI is also effective to detect moderate and advanced fibrosis [10–13].

The purpose of our study was to assess the potential of noninvasive DWI to detect changes in liver diffusion in benign and malignant distal bile duct obstruction, and to investigate the influence of the choice of different b-values.

Materials and methods

Patients

This retrospective study was approved by our institutional review board, and informed consent was waived.

Between May 2011 and March 2012, 92 patients who suspected biliary obstruction underwent magnetic resonance cholangiopancreatography (MRCP), and abdominal MRI, including DWI were enrolled in the study. Patients with cirrhotic liver disease, focal liver lesions, or significant fatty changes in the liver segment (signal drop of >50% on in/on out of phase T1-weighted imaging) were excluded. Patients with intrahepatic and hilar bile duct obstruction or underwent biliary interventional procedures were also excluded. The final study population included 30 patients with distal biliary bile duct obstruction and showed dilatation of the extrahepatic bile duct at MRI. The mean diameter of the common bile duct measured at MRI was 15.7 mm (range 8-25 mm). They were treated surgically or with retrograde cholangiopancreatography in our hospital. Sixteen patients (9 men, 7 women; mean age 64 ± 12 years, range 50-80 years) with malignant distal bile duct obstruction and 14 patients (6 men, 8 women; mean age 66 ± 16 years, range 19-82 years) with benign distal bile duct obstruction were included in our study. The main symptom was jaundice and the mean duration of the symptom was 18 days (range 7-30 days) in patients with malignant bile duct obstruction, whereas the main complaint was abdominal or epigastric pain in patients with benign distal bile duct obstruction and the mean duration of the symptom was 12 days (1-20 days), except 1 patient with distal bile duct stricture who had epigastric pain about 6 months and 2 patients with retained stones following cholecystectomy who had abdominal pain for about 9 months. The control group included 16 patients (3 men, 13 women; mean age 59 ± 18 years, range 19-77 years) whose laboratory, MRCP, and MRI findings for the liver, bile duct, and pancreas were normal. In all 16 malignant lesions, a final diagnosis was made on the basis of histopathological findings after biopsy or surgery; these included pancreatic carcinoma (n = 4), ampullary carcinoma (n = 4), periampullary carcinoma (n = 3), bile duct carcinoma (n = 3), and duodenal carcinoma (n = 2). Of the patients with benign distal obstruction on retrograde cholangiopancreatography, 1 had distal bile duct stricture due to chronic pancreatitis, 13 patients had distal bile duct stones. Of these 13 patients, 5 had retained stones following cholecystectomy.

MRI Protocol

Magnetic resonance imaging was performed with a 1.5-T body system (Avanto; Siemens, Erlangen, Germany) with a 33-mT/m maximum gradient strength. A 12-element phased-array body coil was used. Axial, coronal turbo-spin echo T2-weighted, axial T2 turbo-spin echo with fat saturated, 2D gradient-echo T1-weighted in phase and out phase; and axial, breath-hold 3D gradient-echo T1-weighted with fat saturation sequences before and after the administration of intravenous gadolinium (0.1 mmol/kg bolus) were acquired. Before intravenous contrast material was used, axial abdominal DWIs were performed. We used the same orientation and plane in the routine sequences. A free-breathing single-shot echo-planar-imaging sequence with a chemical shift selective fat-suppression technique was acquired. Sequence parameters were repetition time (TR)/echo time (TE), 4500/88 ms; matrix, 132 × 192; field of view, 350-400 mm; slice thickness, 5 mm; interslice gap, 20% (1 mm); slice numbers, 24-38; echo train length (EPI factor) 156; and 2 excitations. The acquisition time was approximately 4 min, sensitivity-encoding factor was 2, and parallel acquisition imaging (generalized autocalibrating partially parallel

acquisition) with modified sensitivity encoding was applied. The motion-probing gradients were acquired in 3 directions. DWI was performed with b-factors of 200, 600, 800, and 1000 s/mm^2, and the ADC map was generated automatically with the built-in software of the MRI unit.

Multishot thin slab MRCP was also performed. Thick single-slice turbo spin-echo MRCP images were used as reference images and were obtained in the coronal plane. The imaging parameters of MRCP were TR/TE, 3500/383; flip angle, 140°; section thickness with no gap, 50 mm; FOV, 38 cm; matrix, 153 × 256; and acquisition time, 4.5 seconds.

Image Analysis

The postprocessing of DWI datasets was carried out on a Leonardo console (software version 2.0; Siemens), and the ADC maps were reconstructed. A circular regions of interest (ROI) approximately 1-1.5 cm in diameter was placed in 4 segments of the liver (left lobe lateral and medial, and right lobe anterior and posterior segments) to measure ADC values [12]. For ADC values of liver segments, 3 ROIs were placed on each segment and calculated the arithmetic average. We paid attention to exclude vessels and motion artifacts from ROIs. Two examples of our cases are presented in Figures 1 and 2.

Blood Biochemical Results

Serum total and direct bilirubin levels, alkaline phosphatase, alanine aminotransferase, and aspartate aminotransferase levels were obtained on admission in all patients.

Statistical Analysis

Statistical analysis was conducted using statistical software including SPSS software (version 17.0; SPSS, Chicago, IL, USA). For each continuous variable, Kolmogorov-Smirnov and Shapiro-Wilk tests as well as histograms were used to examine for normality. The groups were compared using a 1-way analysis of variance test for normally distributed data, and the Kruskal-Wallis test was applied for non-normally distributed data. Since the analysis of variance was significant, comparisons were applied using the post hoc and Mann-Whitney *U* tests. Repeated measure analyses were used to examine ADC and other pre-post measures data. A P value of $<.05$ was considered statistically significant.

Results

The results of liver function tests on admission are shown in Table 1.

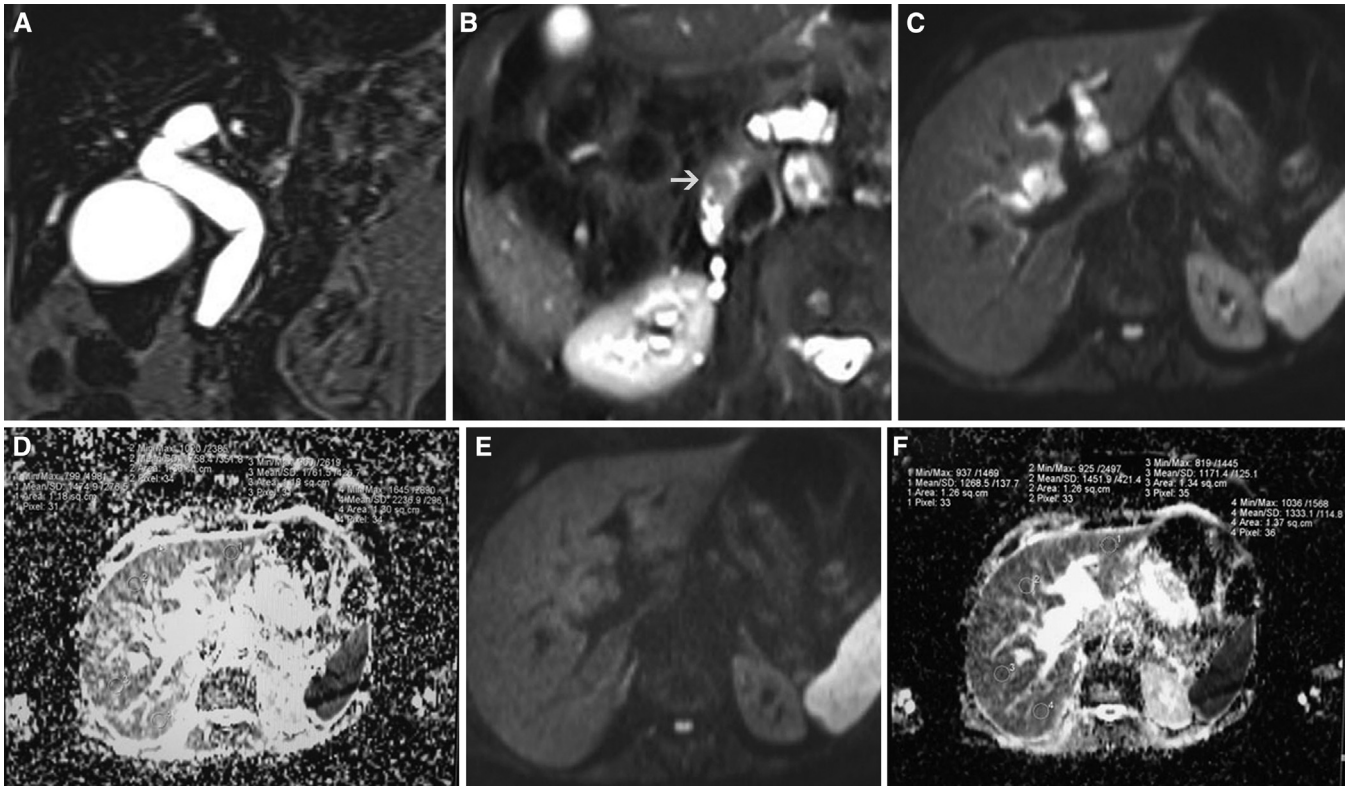

Figure 1. Ampullary carcinoma in a 52-year-old man. (A) Magnetic resonance cholangiopancreatography shows dilatation of gallbladder with abrupt cutoff of common bile duct. (B) Axial T2-weighted magnetic resonance image shows low-intensity lesion at the ampullary region (arrow). (C) Diffusion-weighted image of the liver with a b-factor of 200 s/mm^2, (D) the corresponding ADC image of the liver. The regions of interest are in the 4 segments of the liver. Minimum, maximum, and mean ADC values and standard deviations are seen. (E) Diffusion-weighted image of the liver with a b-factor of 600 s/mm^2, (F) the corresponding apparent diffusion coefficient (ADC) image of the liver. The regions of interest are in the 4 segments of the liver. Minimum, maximum and mean ADC values and standard deviations are seen.

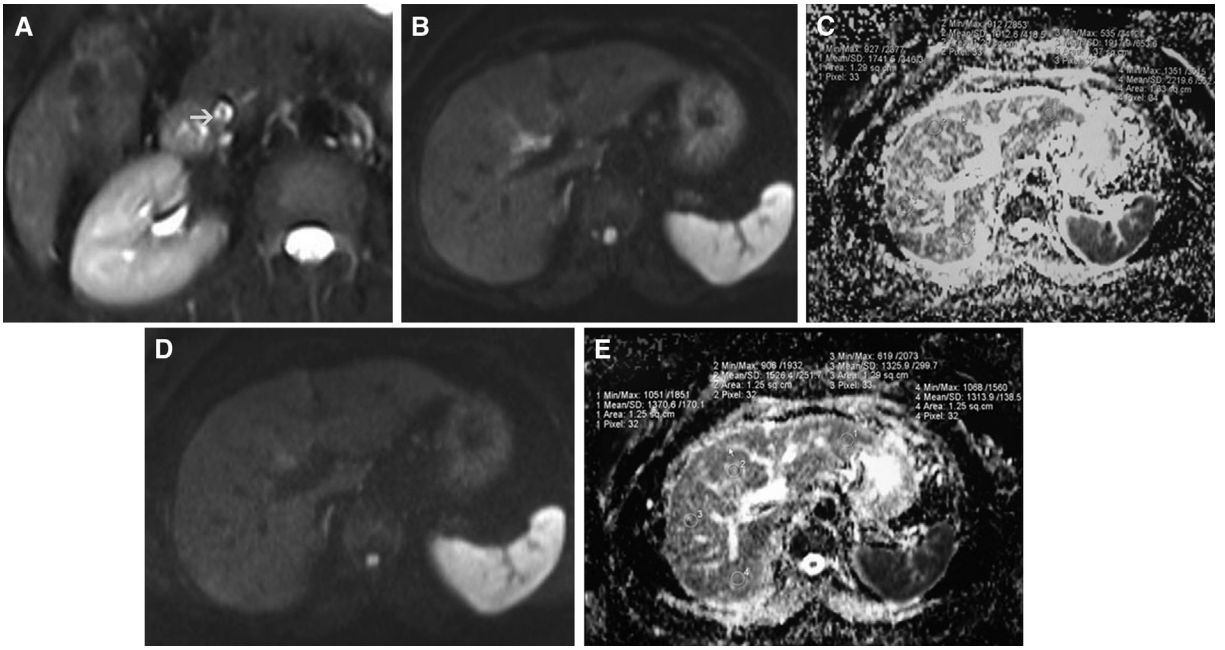

Figure 2. Bile duct stone in a 55-year-old-woman. (A) Axial T2-weighted magnetic resonance image shows distal calculus (arrow). (B) Diffusion-weighted image of the liver with a b-factor of 200 s/mm^2, the corresponding apparent diffusion coefficient (ADC) image of liver (C). The regions of interest are in the 4 segments of the liver. Minimum, maximum, and mean ADC values and standard deviations are seen. (D) Diffusion-weighted image of the liver with a b-factor of 600 s/mm^2, (E) the corresponding ADC image of the liver. The regions of interest are in the 4 segments of the liver. Minimum, maximum, and mean ADC values and standard deviations are seen.

The serum total and direct bilirubin levels, alkaline phosphatase, alanine aminotransferase and aspartate aminotransferase levels were significantly higher in the malignant and benign obstructive groups than those control group ($P < .05$). The serum total and direct bilirubin levels and alkaline phosphatase level were significantly higher in the malignant obstuctive group than those benign obstructive group ($P < .05$). The serum alanine aminotransferase and aspartate aminotransferase levels did not differ significantly between the patients with malignant obstructive and benign obstructive group ($P > .05$). There were no correlations between the ADC values of liver segments and liver function tests.

Table 1
Comparison of liver function test between 3 groups

Group	ALT (IU/L)	AST (IU/L)	Total bilirubin (mg/dL)	Direct bilirubin (mg/dL)	ALP (IU/L)
Malignant (n = 16)					
Mean	168.7	116.1	11.5	8.4	366.3
Median	120.0	84.0	12.6	9.1	311.0
Minimum	23.0	42.0	0.5	0.1	105.0
Maximum	812.0	282.0	25.9	23.8	912.0
Benign (n = 14)					
Mean	188.9	176.3	2.6	2.0	224.8
Median	107.5	82.5	2.0	1.2	168.5
Minimum	10.0	17.0	0.4	0.1	57.0
Maximum	833.0	886.0	11.8	10.6	761.0
Control (n = 16)					
Mean	20.6	23.1	0.4	0.1	74.5
Median	21.5	18.5	0.4	0.1	72.5
Minimum	12.0	15.0	0.4	0.1	56.0
Maximum	31.0	47.0	0.6	0.2	100.0
P	**.021**	**.017**	**.0001**	**.0001**	**.0001**

Kruskal-Wallis test was used. Significant differences ($P < .05$) are in bold font.
ALP = alkaline phosphatase; ALT = alanine aminotransferase; AST = aspartate aminotransferase.

Results of the ADC value comparison of liver segments in the obstruction and control groups are shown in detail in Table 2.

The mean ADC values of liver segments in the malignant group were significantly lower than in the benign obstructive and control groups using a b-value of 200 s/mm^2 ($P < .05$) (Figure 3). However, there were no significant differences in ADC values for the benign obstructive and control groups. The mean ADC values of the left lobe medial and lateral segments were significantly lower in the malignant obstruction group than in the benign obstructive and control groups using a b-value of 600 s/mm^2 ($P < .05$) (Figure 4). There were no significant differences between groups in mean ADC values for the right posterior and anterior segments using a b-value of 600 s/mm^2 ($P > .05$). Using a b-value of 800 s/mm^2, ADC values of all 4 liver segments in each group were not significantly different ($P > .05$). The ADC values of the right lobe posterior segment were significantly lower in the malignant and benign obstruction groups than in the control group using a b-value of 1000 s/mm^2 ($P < .05$).

Discussion

Chronic biliary obstruction may result in hepatic fibrosis and secondary biliary cirrhosis [3,14,15]. In a study of bile-ligated rats, biliary cirrhosis was occurred in all living animals after 4 weeks [16]. In another experimental study, extrahepatic

Table 2
Comparison of mean ADC values of liver segments between 3 groups

GROUPS	ADC (LL)	ADC (LM)	ADC (RA)	ADC (RP)
b = 200 s/mm^2				
Malignant (n = 16)	1.6 ± 0.3	1.8 ± 0.3	1.8 ± 0.2	1.9 ± 0.3
Benign (n = 14)	2.3 ± 0.7	2.2 ± 0.4	2.1 ± 0.5	2.2 ± 0.5
Control (n = 16)	2.6 ± 0.5	2.4 ± 0.3	2.4 ± 0.5	2.4 ± 0.3
P	**.0001**	**.0001**	**.001**	**.002**
b = 600 s/mm^2				
Malignant (n = 16)	1.4 ± 0.2	1.3 ± 0.2	1.3 ± 0.,2	1.4 ± 0.2
Benign (n = 14)	1.6 ± 0.3	1.5 ± 0.2	1.4 ± 0.2	1.3 ± 0.4
Control (n = 16)	1.7 ± 0.3	1.5 ± 0.2	1.4 ± 0.2	1.5 ± 0.2
P	**.009**	**.035**	.099	.137
b = 800 s/mm^2				
Malignant (n = 16)	1.3 ± 0.3	1.3 ± 0.2	1.2 ± 0.2	1.3 ± 0.2
Benign (n = 14)	1.4 ± 0.2	1.3 ± 0.2	1.1 ± 0.3	1.2 ± 0.2
Control (n = 16)	1.5 ± 0.2	1.3 ± 0.2	1.3 ± 0.1	1.4 ± 0.2
P	.073	.448	.222	.299
b = 1000 s/mm^2				
Malignant (n = 16)	1.2 ± 0.3	1.1 ± 0.2	1.1 ± 0.2	1.1 ± 0.3
Benign (n = 14)	1.2 ± 0.3	1.2 ± 0.2	1.0 ± 0.1	1.1 ± 0.2
Control (n = 16)	1.3 ± 0.1	1.2 ± 0.2	1.1 ± 0.1	1.3 ± 0.1
P	.227	.152	.144	**.029**

Kruskal-Wallis test was used. Significant differences ($P < .05$) are in bold font. ADC = apparent diffusion coefficient; LL = left lobe lateral; LM = left lobe medial; RA = right lobe anterior; RP = right lobe posterior.

cholestasis induced intensified bile duct proliferation and fibrosis 4 weeks after surgery [17]. Hammel et al [18] reported secondary biliary cirrhosis as early as 12 weeks after "diagnosis" of bile duct obstruction associated with chronic pancreatitis. Early-stage liver fibrosis can be treated in humans [18–20].

MRI or MRCP are able to show dilatation of the bile duct down to the level of the periampullary region in many benign

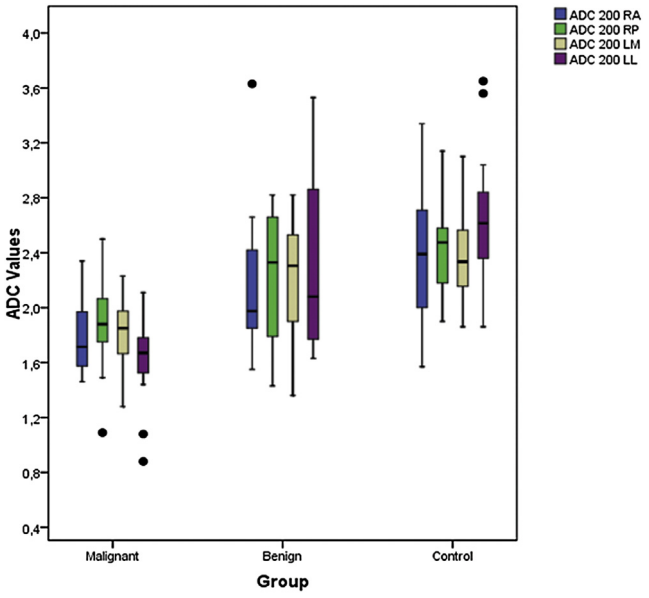

Figure 3. Box and whisker plots showing apparent diffusion coefficient (ADC) values of each groups. The middle line in each box shows the median. The whiskers represent the range from the maximum to the minimum calculated ADC values. 0 = outlier. The unit of ADC value is $\times 10^{-3}$ mm^2/s. ADC200, ADC with b factor of 200. LL = left lobe lateral; LM = left lobe medial; RA = right lobe anterior; RP = right lobe posterior. This figure is available in colour online at http://carjonline.org/.

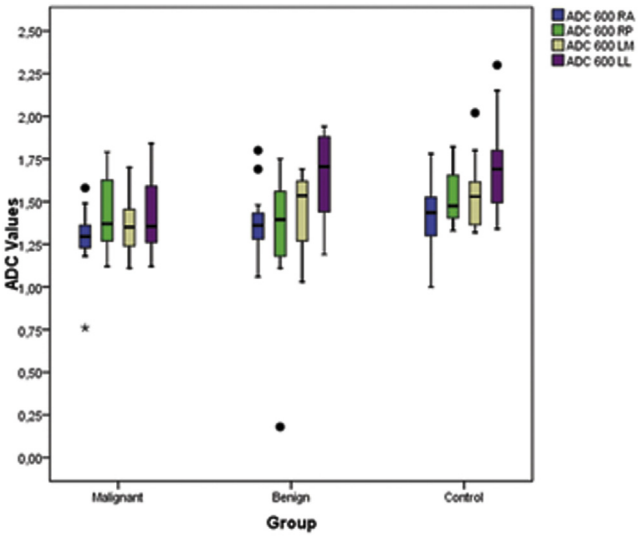

Figure 4. Box and whisker plots showing apparent diffusion coefficient (ADC) values of each groups. The middle line in each box shows the median. The whiskers represent the range from the maximum to the minimum calculated ADC values. 0 = outlier. The unit of ADC value is $\times 10^{-3}$ mm^2/s. ADC600, ADC with b factor of 600. LL = left lobe lateral; LM = left lobe medial; RA = right lobe anterior; RP = right lobe posterior. This figure is available in colour online at http://carjonline.org/.

and malignant lesions. However, the differentiation between malignant and benign lesions in the periampullary regions is difficult using MRI or MRCP because of an overlap in imaging features [21,22]. Park et al [23] reported that benign strictures frequently showed hypervascularity on arterial and portal venous phase images, similar to malignant strictures. Few studies have investigated DWI for the evaluation of cholestasis. Hashimoto et al [5] found that increased signal intensity on T1-weighted images in the ductal dilatation area is due to ductular proliferation, bile pigments within the hepatocytes, and periportal fibrosis with inflammatory cell infiltration histologically. He suggested that cholestasis is main determinant factor for segmental high intensity areas on T1-weighted images patients with intrahepatic ductal dilation. Tam et al's [6] study of 21 patients with malignant bile duct obstruction found that concomitantly high T1-weighted and DWI signals in liver segments was associated with lower ADC values, which might indicate underlying cellular damage. Various studies have shown that ADC values in cirrhotic livers are lower than in normal livers [10–13]. However, the mechanisms of diffusion restriction in cirrhotic livers are incompletely understood. It is most likely due to increased quantity of connective tissue in the liver and decreased blood flow [10,11].

Previous studies reported that the choice of b-value affects the calculated ADC [24–27]. High b-values (≥500 s/mm^2) are sensitive to diffusion and provide small ADC values to prevent perfusion effects in ADC measurements [26,27]. Soylu et al [24] and Hollingsworth and Lomas [25] conduct that calculating ADC values from the right lobe posterior segment using high b-values (500-750 s/mm^2) limited the changes in perfusion and prevented artifacts caused by cardiac and intestinal motions in the left lobe of the liver. Thus, liver

fibrosis could be better evaluated. However, Girometti et al [27] provided that calculating ADC values using an intermediate b-value of 400 s/mm^2 as opposed to a higher b-value of 800 s/mm^2 may be an advantage in the evaluation of hepatic fibrosis. There was no clinically significant difference between ADC values of cirrhotic and normal livers at b = 800 s/mm^2. In another study, liver fibrosis was measured by using b-values of 200 and 400 have provided better results [28].

We performed the measurement of ADC values in 4 segments of the liver and used multiple b-values. Similarly, in our study, when a b-value of 800 s/mm^2 was used, there were no significant differences between liver segments or groups. However, we did find that ADC values of the right lobe posterior segment were significantly lower in malignant and benign obstruction groups than in the control group using a b-value of 1000 s/mm^2 ($P < .05$). Previous studies have also reported that when low b-values are used, ADC values are more strongly affected by perfusion [24,25,27,28]. Biliary tract obstruction can result in around a 40% decrease in total hepatic blood flow [29]. Moteki and Horikoshi [30] suggested that proximal hepatic arterial stenosis and/or biliary tract obstruction decreased liver perfusion. Annet et al [31] demonstrated that ADC values decreased in rats with hepatic fibrosis, but not after death. The ADC differences in dead and living rats were related to perfusion effects. Compared to healthy subjects, patients with cirrhosis or fibrosis exhibit substantially reduced hepatic perfusion. In one 2008 study, the restricted diffusion detected in patients with cirrhosis was mainly related to decreased diffusion-related perfusion [32]. Sandrasegaran et al [33] found that lower b-values (50-400 s/mm^2) are more sensitive to the effects of perfusion and may allow better discrimination of hepatic fibrosis stage. In our study, we found that mean ADC values were significantly lower in the malignant obstruction group than in the benign obstruction or control groups using a b-value of 200 s/mm^2. We also found no significant differences in ADC values of the benign obstruction and control groups. Using a b-value of 600s/mm^2, the mean ADC values of the left lobe medial and lateral segments were significantly lower in the malignant obstruction group than in the benign obstructive or control group.

It is possible that the time of obstruction is a factor affecting liver diffusion and perfusion. Malignant obstruction may take some weeks, whereas bile duct stones can cause jaundice in hours or a few days. In our study, the mean duration of the obstruction in the malignant obstructive group was longer than that of benign obstructive group except 3 patients. The serum alanine aminotransferase and aspartate aminotransferase levels did not differ significantly between the patients with malignant obstructive and benign obstructive group ($P > .05$). However, the poor correlation between transaminase levels and the degree of liver injury has been reported in a previous study [6]. However, the serum total and direct bilirubin levels and alkaline phosphatase level were significantly higher in the malignant obstructive group than those in the benign obstructive group. These results indicate a marked pressure increase in the bile ducts of the malignant obstructive group. Complete obstruction of the bile duct with a mass may result in a markedly increased cholestasis. Moreover, decreased hepatic blood flow and increased portal pressure due to obstruction may cause hypoxia/ischemic damage liver paranchyma and bile duct. These features may increase cholestasis as reported by previous studies [34,35]. Matsumoto et al [34] suggested that the reduction in the number of fenestrae in the liver sinusoidal endothelial cells may lead to dysfunction of the liver microcirculation in the common bile ligated rats. Hypoxia/ischemia in the tissue may also directly induce an inflammatory response or promote expression vascular endothelial growth factor, which causes bile duct proliferation [35].

In present study, using b-values of 200 and 600 s/mm^2, lower ADC values in livers with malignant obstruction may be explained by a marked depression in hepatic microcirculation, a long period of hepatocyte damage, inflammation. These findings may assist in the differentiation between long-term malignant obstruction and acute benign distal bile duct obstruction. In addition, we did find that ADC values of the right lobe posterior segment were significantly lower in malignant and benign obstruction groups than in the control group using a b-value of 1000 s/mm^2. These finding may be due to an inflammatory response and bile duct proliferation in liver paranchyma.

Our study had some limitations. First, we did not undertake pathological examinations of the liver. In routine clinical practice, a liver biopsy should not be performed in patients with biliary obstruction. Second, the subject groups were relatively small. Third, biliary stones were the cause of obstruction in patients of benign distal biliary obstruction.

Conclusion

In conclusion, our study showed that DWI can be beneficial for detection of changes in liver diffusion in patients with bile duct obstruction. We showed that the choice of b-value does affect the calculated ADC. In this study, b-values of 200 and 600 give better results for detection of changes on the liver paranchyma in patients with obstructive jaundice. The measurement of ADC values of liver segments may be useful in the characterisation of distal bile duct obstruction. Further prospective studies involving larger samples, preferably including patients who have undergone liver biopsy and DWI, are needed to evaluate the correlation between ADC values and histological findings.

References

[1] Sheen JM, Huang LT, Hsieh CS, Chen CC, Wang JY, Tain YL. Bile duct ligation in developing rats: temporal progression of liver, kidney, and brain damage. J Pediatr Surg 2010;45:1650–8.

[2] Karan B, Kama NA, Hascelik G, Ercan M. Effects of vitamin A on immunological deficiencies in rats with obstructive jaundice. Eur J Surg 1996;162:217–22.

[3] Aller MA, Arias JL, Prieto I, Losada M, Arias J. Bile duct ligation: step-by-step to cholangiocyte inflammatory tumorigenesis. Eur J Gastroenterol Hepatol 2010;22:651–61.

[4] Copple BL, Jaeschke H, Klaassen CD. Oxidative stress and the pathogenesis of cholestasis. Semin Liver Dis 2010;30:195–204.
[5] Hashimoto M, Akabane Y, Heianna J, et al. Segmental high intensity on T1-weighted hepatic MR images. Abdom Imaging 2005;30:60–4.
[6] Tam HH, Collins DJ, Wallace T, Brown G, Riddell A, Koh DM. Segmental liver hiperintensity in malignant biliary obstruction on diffusion weighted MRI: associated MRI findings and relationship with serum alanine aminotransferase levels. Br J Radiol 2012;85:22–8.
[7] Thoeny HC, Binser T, Roth B, Kessier TM, Vermanthen P. Noninvasive assessment of acute ureteral obstruction with diffusion-weighted MR imaging. Radiology 2009;252:721–8.
[8] Culverwell AD, Sheridan MB, Guthrie JA, Scarsbrook AF. Diffusion-weighted MRI of the liver - Interpretative pearls and pitfalls. Clin Radiol 2013;68:406–14.
[9] Di Pietropaolo M, Briani C, Federici GF, et al. Comparison of diffusion-weighted imaging and gadoxetic acid-enhanced MR images in the evaluation of hepatocellular carcinoma and hypovascular hepatocellular nodules. Clin Imaging 2015;39:468–75.
[10] Taouli B, Koh DM. Diffusion-weighted MR imaging of the liver. Radiology 2010;254:47–66.
[11] Chiaradia M, Baranes L, Pigneur F, et al. Liver magnetic resonance diffusion weighted imaging: 2011 update. Clin Res Hepatol Gastroenterol 2011;35:539–48.
[12] Bakan AA, Inci E, Bakan S, Gokturk S, Cimilli T. Utility of diffusion-weighted imaging in the evaluation of liver fibrosis. Eur Radiol 2012;22:682–7.
[13] Taouli B, Ehman RL, Reeder SB. Advanced MRI methods for assessment of chronic liver disease. AJR Am J Roentgenol 2009;193:14–27.
[14] Sener G, Kabasakal L, Yuksel M, Gedik N, Alican Y. Hepatic fibrosis in biliary-obstructed rats is prevented by ginkgo biloba treatment. World J Gastroenterol 2005;11:5444–9.
[15] Sanchez-Patan F, Anchuelo R, Corcuera MT, et al. Biliary fibrosis in microsurgical extrahepatic cholestasis in the rat. Microsurgery 2008;28:361–6.
[16] Kountouras J, Billing BH, Scheuer PJ. Prolonged bile duct obstruction: a new experimental model for cirrhosis in the rat. Br J Exp Path 1984;65:305–11.
[17] Aller MA, Duran M, Ortega L, et al. Comparative study of macro-microsurgical extrahepatic cholestasis in the rat. Microsurgery 2004;24:442–7.
[18] Hammel P, Couvelard A, O'Tootle D, et al. Regression of liver fibrosis after biliary drainage in patients with chronic pancreatitis and stenosis of common bile duct. N Engl J Med 2001;344:418–23.
[19] Ibrarullah M, Sikora SS, Agarwal DK, Kapoor VK, Kaushik SP. 'Latent' portal hypertension in benign biliary obstruction. HPB Surg 1996;9:149–52.
[20] Sikora SS, Srikanth G, Agrawal V, Gupta RK, Kumar A, Saxena R. Liver histology in benign biliary stricture: fibrosis to cirrhosis … and reversal? J Gastroenterol Hepatol 2008;23:1879–84.
[21] Kim JH, Kim MJ, Chung JJ, Lee WJ, Yoo HS, Lee JT. Differential diagnosis of periampullary carcinomas at MR imaging. Radiographics 2002;22:1335–52.
[22] Kim TU, Kim S, Lee JW, et al. Ampulla of Vater: comprehensive anatomy, MR imaging of pathologic conditions, and correlation with endoscopy. Eur J Radiology 2008;66:48–64.
[23] Park HJ, Kim SH, Jang KM, Choi SY, Lee SJ, Choi D. The role of diffusion-weighted MR imaging for differentiating benign from malignant bile duct strictures. Eur Radiol 2014;24:947–58.
[24] Soylu A, Kılıçkesmez Ö, Poturoğlu Ş, et al. Utility of diffusion-weighted MRI for assessing liver fibrosis. Diagn Interv Radiol 2010;16:204–8.
[25] Hollingsworth KG, Lomas DJ. Influence of perfusion on hepatic MR diffusion measurement. NMR Biomed 2006;19:231–5.
[26] Taouli B, Tolia AJ, Losada M, et al. Diffusion-weighted MRI for quantification of liver fibrosis: preliminary experience. AJR Am J Roentgenol 2007;189:799–806.
[27] Girometti R, Furlan A, Esposito G, Bazzocchi M, Como G, Soldano F. Relavence of b-values in evaluating liver fibrosis: a study in healthy and cirrhotic subjects using two single-shot spin-echo echo-planar diffusion-weighted sequences. J Magn Reson Imaging 2008;28:411–9.
[28] Aube C, Racineux PX, Lebigot J, et al. Diagnosis and quantification of hepatic fibrosis with diffusion weighted MR imaging: preliminary results. J Radiol 2004;85:301–6.
[29] Mathie RT, Nagomey DM, Lewis MH, Blumgart LH. Hepatic hemodynamics after chronic obstruction of the biliary tract in the dog. Surg Gynecol Obstet 1988;166:125–30.
[30] Moteki T, Horikoshi H. Evaluation of noncirrhotic hepatic parenchyma with and without significant portal vein stenosis using diffusion-weighted echo-planar MR on the basis of multiple-perfusion-components theory. Magn Reson Imaging 2011;29:64–73.
[31] Annet L, Peeters F, Abarca-Quinones J, Leclercq I, Moulin P, Van Beers BE. Assessment of diffusion-weighted MR imaging in liver fibrosis. J Magn Reson Imaging 2007;25:122–8.
[32] Luciani A, Vignaud A, Cavet M, et al. Liver cirrhosis: intravoxel incoherent motion MR imaging-pilot study. Radiology 2008;249:891–9.
[33] Sandrasegaran K, Akisik FM, Lin C, et al. Value of diffusion-weighted MRI for assessing liver fibrosis and cirrhosis. AJR Am J Roentgenol 2009;193:1556–60.
[34] Matsumoto Y, Nimoto S, Katayama K, Hirose K, Yamaguchi A, Torigoe K. Effects of biliary drainage in obstructive jaundice on microcirculation, phagocytic activity, and ultrastructure of the liver in rats. J Hepatobiliary Pancreat Surg 2002;9:360–6.
[35] Toki F, Takahashi A, Suzuki M, Ootake S, Hirato J, Kuwano H. Development of an experimental model of cholestasis induced by hypoxic/ischemic damage to the bile duct and liver tissues in infantile rats. J Gastroenterol 2011;46:639–47.